

## Relation between exchange anisotropy and magnetization reversal asymmetry in Fe/MnF<sub>2</sub> bilayers

I. N. Krivorotov,<sup>1</sup> C. Leighton,<sup>2</sup> J. Nogués,<sup>3</sup> Ivan K. Schuller,<sup>4</sup> and E. Dan Dahlberg<sup>1</sup>

<sup>1</sup>*Department of Physics, University of Minnesota, 116 Church Street SE, Minneapolis, Minnesota 55455*

<sup>2</sup>*Department of Chemical Engineering and Materials Science, University of Minnesota, 421 Washington Avenue SE, Minneapolis, Minnesota 55455*

<sup>3</sup>*Institució Catalana de Recerca i Estudis Avançats (ICREA) and Department de Física, Universitat Autònoma de Barcelona, 08193 Bellaterra, Spain*

<sup>4</sup>*Department of Physics, University of California–San Diego, La Jolla, California 92093-0319*

(Received 28 August 2001; published 12 February 2002)

The angular dependence of the magnetic anisotropy of exchange biased Fe/MnF<sub>2</sub> bilayers was measured. Below the Néel temperature of the antiferromagnetic MnF<sub>2</sub> layer, an exchange anisotropy is observed which consists of unidirectional, uniaxial, threefold and fourfold symmetry components. The threefold exchange anisotropy term is responsible for the asymmetric magnetization reversal process recently observed in this system.

DOI: 10.1103/PhysRevB.65.100402

PACS number(s): 75.70.Cn, 73.50.Jt, 75.30.Gw

Although exchange coupling between ferromagnets (F) and antiferromagnets (AF) was discovered forty-five years ago,<sup>1</sup> a quantitative understanding of this phenomenon is still lacking (see Ref. 2 for a review). Two of the defining characteristics of this effect are an enhancement of the coercivity and a shift of the hysteresis loop along the axis defined by a cooling field. Both characteristics only occur below the Néel temperature of the antiferromagnet ( $T_N$ ). In recent years, exchange bias has attracted considerable attention in part due to its technological applications.<sup>3</sup> In general, it is well established that the shape of a hysteresis loop depends on the mechanism of the magnetization reversal process, however, until recently,<sup>4–7</sup> little was known about this process in exchange biased systems. The recent polarized neutron reflectometry<sup>5</sup> and magnetoresistance<sup>8</sup> studies of Fe/MnF<sub>2</sub> bilayers revealed that the magnetization reversal of Fe layer is asymmetric below  $T_N$  of MnF<sub>2</sub> ( $T_N=67$  K). This work established that the magnetization states at the two coercive fields of the hysteresis loop are different. At the coercive field opposite to the easy direction of exchange bias (left coercive field) the magnetization is perpendicular to the applied field direction. This is to be contrasted to the state of magnetization at the coercive field in the easy direction of exchange bias (right coercive field), which consists of domains that are parallel and antiparallel to the applied field.

In the present work, we have studied both the anisotropy energies and the magnetization reversal process using the anisotropic magnetoresistance (AMR) as a probe of the magnetic state.<sup>9,10</sup> We found that the anisotropy energy has a complex dependence on the in-plane direction of the F layer magnetization. More precisely, it consists of unidirectional, uniaxial, threefold and fourfold (biaxial) symmetry components. We also found that in the presence of an applied magnetic field, this complex anisotropy results in the asymmetric magnetization reversal.<sup>5</sup>

We have studied three Fe/MnF<sub>2</sub> bilayers prepared by electron beam evaporation. First, a 25 nm thick buffer layer of ZnF<sub>2</sub> was grown on a (100) MgO substrate followed by a 65

nm thick layer of MnF<sub>2</sub>. Then, a 12 nm Fe layer was deposited on the MnF<sub>2</sub> layer followed by a cap layer of Al (10 nm). The x-ray diffraction data showed that the MnF<sub>2</sub> layer was twinned quasiepitaxial, and the Fe layer was polycrystalline. Both crystal domains (twins) of the MnF<sub>2</sub> film have their (110) planes parallel to the (100) plane of the MgO substrate; the [001] directions of the twins make a 45° angle with the [001] direction of the substrate.<sup>11</sup> The AF easy axes of both twins are in the plane of the sample at 45° to the [001] direction of the MgO substrate. Previous studies have shown that the sign and the magnitude of the hysteresis loop shift in Fe/MnF<sub>2</sub> bilayers depend on the magnitude of the cooling field,<sup>11</sup> exhibiting a positive exchange bias effect in large fields.<sup>12</sup> For measurements reported in this paper, a cooling field of 1 kOe was applied along the [001] direction of the MgO substrate resulting in a negative exchange bias.

Figure 1 shows a superconducting quantum interference device magnetometry hysteresis loop [Fig. 1(a)] and a magnetoresistance loop [Fig. 1(b)] as the field is swept from 300 Oe to -300 Oe and back along the cooling field direction. The difference in magnetization reversal mechanisms for the

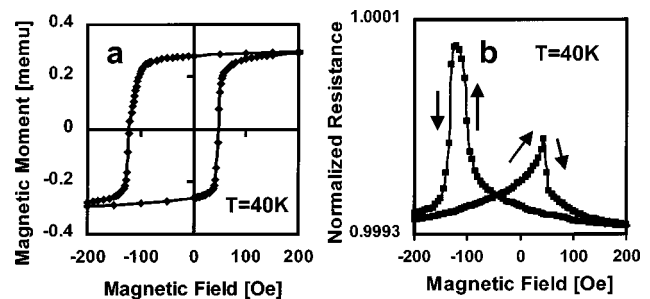


FIG. 1. (a) Magnetization and (b) magnetoresistance hysteresis loops of Fe/MnF<sub>2</sub> measured along the [001] crystallographic direction of the MgO substrate at 40 K for the cooling field magnitude of 1 kOe; the lines are guides to the eye. The asymmetry of magnetization reversal mechanism is evident from the magnetoresistance plot (see text).

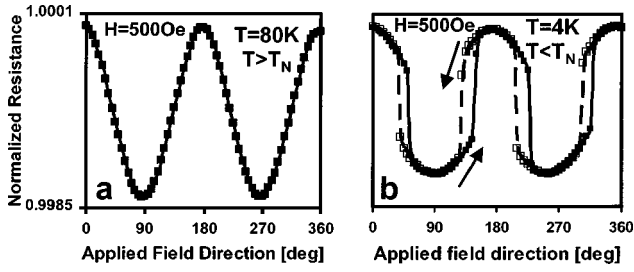


FIG. 2. Dependence of the resistance on the angle between the current and an applied field of 500 Oe for the Fe/MnF<sub>2</sub> bilayer at 80 K (a) and 4.2 K (b); the lines are guides to the eye. The jumps in the resistance in (b) indicate the fourfold anisotropy induced below  $T_N$  of the MnF<sub>2</sub>.

two branches of the hysteresis loop is not obvious from the magnetometry measurements [Fig. 1(a)], however, it is clearly seen in the magnetoresistance data [Fig. 1(b)]. The variation in the resistance is due to the AMR, which depends upon the angle the magnetization makes with the current. For Fe, the maximum value of resistance is observed for the magnetization parallel or antiparallel to the current direction. For the data shown in Fig. 1(b), the current is perpendicular to the applied magnetic field, thus the resistance is at a minimum for saturating magnetic fields of  $\pm 300$  Oe. For the decreasing field sweep, the resistance passes through a maximum. Comparing the value of this peak resistance to the AMR magnitude indicates that magnetization of the sample is mostly perpendicular to the applied field. However, the peak for the increasing field sweep is much smaller indicating that magnetization is breaking up onto domains that are mostly parallel and antiparallel to the applied field.

A technique utilizing the AMR to determine the magnetization direction<sup>9</sup> was used for our studies of the angular dependence of exchange anisotropy energy. For polycrystalline ferromagnets, the AMR is given by

$$R = R_0 + \Delta R \cdot \cos^2(\alpha_M). \quad (1)$$

Here  $\alpha_M$  is the angle between the current and the magnetization. Figure 2(a) demonstrates that the AMR of our Fe/MnF<sub>2</sub> sample at  $T = 80\text{ K}$  ( $T > T_N$ ) is well described by Eq. (1) for the applied field of 500 Oe. However, the angular dependence of the resistance in the same external field of 500 Oe is significantly modified at  $T = 4.2\text{ K}$  [Fig. 2(b)]. There are four jumps in the plot of the resistance versus applied field direction that result from the transition of the magnetization from one of the four local energy minima that develop below  $T_N$  to another. This behavior is a clear signature of the strong fourfold anisotropy induced by the exchange interaction between the Fe and MnF<sub>2</sub> layers.

In equilibrium, the torque per area,  $\tau$ , acting on the Fe magnetization due to magnetic anisotropy of the sample is equal in magnitude to the torque due to the external magnetic field. The magnitude of  $\tau$  is given by

$$\tau(\alpha_M) = H \cdot M \cdot t_F \cdot \sin(\alpha_M - \alpha_H), \quad (2)$$

where  $H$  is the magnitude of the external magnetic field,  $M$  is magnetization of Fe,  $t_F$  is the thickness of the Fe layer,  $\alpha_M$  is

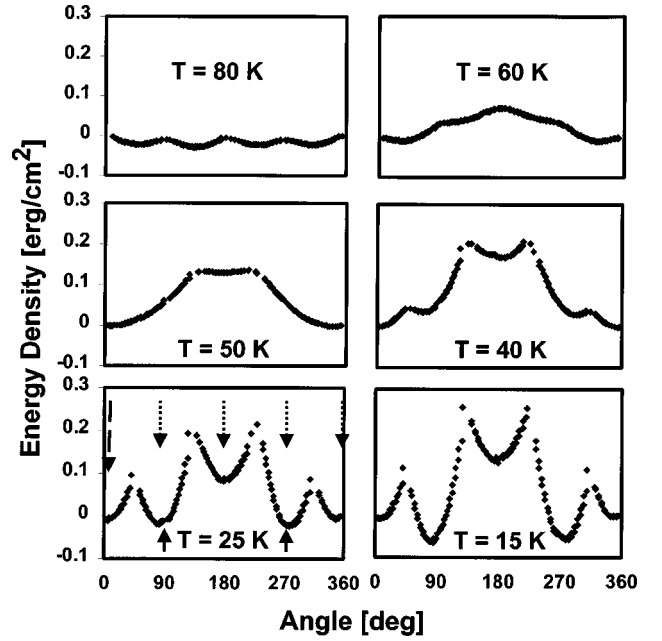


FIG. 3. Experimentally determined exchange anisotropy energy per unit area of the Fe/MnF<sub>2</sub> bilayer as a function of the Fe magnetization direction at six different temperatures. The arrows in the plot for  $T = 25\text{ K}$  indicate the easy directions of biaxial anisotropy (arrows with dotted lines), uniaxial anisotropy (arrows with solid lines) and unidirectional anisotropy (arrow with dashed line).

the angle which describes the magnetization direction, and  $\alpha_H$  is the angle describing the magnetic field direction.

Using the resistance measured while rotating an external magnetic field through  $360^\circ$  in the plane of the sample, one can obtain the direction of magnetization,  $\alpha_M$ , from Eq. (1). With the value of  $\alpha_M$  determined for each value of  $\alpha_H$  and the other known quantities, one can then calculate the torque  $\tau(\alpha_M)$  using Eq. (2). Finally, numerical integration of  $\tau(\alpha_M)$  with respect to  $\alpha_M$  yields the angular dependence of the in-plane magnetic anisotropy energy per area  $K(\alpha_M)$ .

Figure 3 shows  $K(\alpha_M)$  obtained by this method at six different temperatures. For the temperatures above  $T_N$  of MnF<sub>2</sub> (e.g.,  $T = 80\text{ K}$ ), there are small intrinsic biaxial and uniaxial anisotropies that stem from either the texture in the polycrystalline Fe film, or a growth induced anisotropy. As the sample is cooled to a temperature below  $T_N$  (e.g.,  $T = 60\text{ K}$ ,  $T = 50\text{ K}$ ), a unidirectional anisotropy is induced in the sample in addition to the small intrinsic anisotropies of the Fe film. For lower temperatures ( $T = 40\text{ K}$ ,  $T = 25\text{ K}$ ), the exchange coupling also induces a biaxial anisotropy with the hard axes at  $\pm 45^\circ$  to the [001] direction of the substrate, i.e., along the AFM twins. The magnitude of this biaxial anisotropy increases with decreasing temperature and its easy axes coincide with the hard axes of the intrinsic biaxial anisotropy of the Fe layer. Apparently, the easy axis of the FM layer rotates by  $45^\circ$  as the sample is cooled to low temperatures, similar to what is observed for Fe/FeF<sub>2</sub> bilayers.<sup>13</sup> In addition to the unidirectional and the biaxial anisotropies, the exchange coupling between the Fe and MnF<sub>2</sub> results in a

uniaxial anisotropy with its easy axis perpendicular to the unidirectional anisotropy. Similar to our results, exchange induced unidirectional, uniaxial and biaxial anisotropy components were previously observed in epitaxial NiFe/FeMn bilayers.<sup>14</sup>

The origin of the biaxial anisotropy may be attributed to the spin-flop coupling<sup>15,16</sup> and the twinned nature of the MnF<sub>2</sub> film. When the Fe magnetization is at 45° to the easy axes of both MnF<sub>2</sub> twins, the AF spins may cant in both twins resulting in a low energy state. If the Fe magnetization is perpendicular to the AF easy axis of one of the twins and parallel to the AF easy axis of the other, then the AF cant occurs only in the twin with its AF easy axis perpendicular to the Fe magnetization. This results in a hard direction of anisotropy of the system. There are four such hard directions in our system and, therefore, the spin-flop coupling results in a biaxial anisotropy. It was proposed<sup>16</sup> that the spin-flop coupling leads to an increased coercivity in AF/F bilayers. In our system, the coercivity is roughly proportional to the biaxial anisotropy component at all temperatures below  $T_N$ . Thus this result supports the spin-flop origin of the enhanced coercivity in this system.

Figure 4 demonstrates how the exchange anisotropy results in different mechanisms of magnetization reversal for the two branches of the hysteresis loop. The total energy per unit area of the F layer magnetization in the external field applied along the cooling field direction is given by

$$E = K(\alpha) - H \cdot M \cdot t_F \cos(\alpha). \quad (3)$$

Here  $K(\alpha)$ , shown in Fig. 4(a), is the anisotropy energy per area at  $T = 40$  K and  $\alpha$  is the angle between the cooling field and magnetization. Figures 4(b) and 4(c) show the energy given by Eq. (3) as a function of  $\alpha$  at  $T = 40$  K for two particular magnitudes of the applied field  $H = -120$  Oe [Fig. 4(b)] and  $H = 45$  Oe [Fig. 4(c)]. Figure 1(a) shows that these are the coercive fields at 40 K. For the left coercive field [ $-120$  Oe, Fig. 4(b)], the local energy minimum in the cooling field direction ( $0^\circ$ ) disappears and the magnetization rotates away from this direction. There are now two local energy minima at nearly  $90^\circ$  to the applied field direction. Hence, in the reversal process, the magnetization will fall into one of these local minima. However, at the right coercive field [ $45$  Oe, Fig. 4(c)], the energy versus magnetization direction plot does not have local minima between  $0^\circ$  and  $180^\circ$  and thus does not provide a metastable state perpendicular to the cooling field direction.

The solid line in Fig. 4(a) is a fit of the following equation:

$$K(\alpha) = -K_{UD} \cos(\alpha) - K_{UA} \cos(2\alpha) - K_3 \cos(3\alpha) - K_{BA} \cos(4\alpha) \quad (4)$$

to the experimentally measured exchange anisotropy at  $T = 40$  K. In Eq. (4),  $K_{UD}$ ,  $K_{UA}$ ,  $K_3$ , and  $K_{BA}$  are the unidirectional, uniaxial, threefold and biaxial anisotropy constants. The values of the anisotropy constants obtained from this fit are:  $K_{UD} = 0.097$  erg/cm<sup>2</sup>,  $K_{UA} = -0.014$  erg/cm<sup>2</sup>,  $K_3 = -0.01$  erg/cm<sup>2</sup>,  $K_{BA} = 0.023$  erg/cm<sup>2</sup>. It is important to

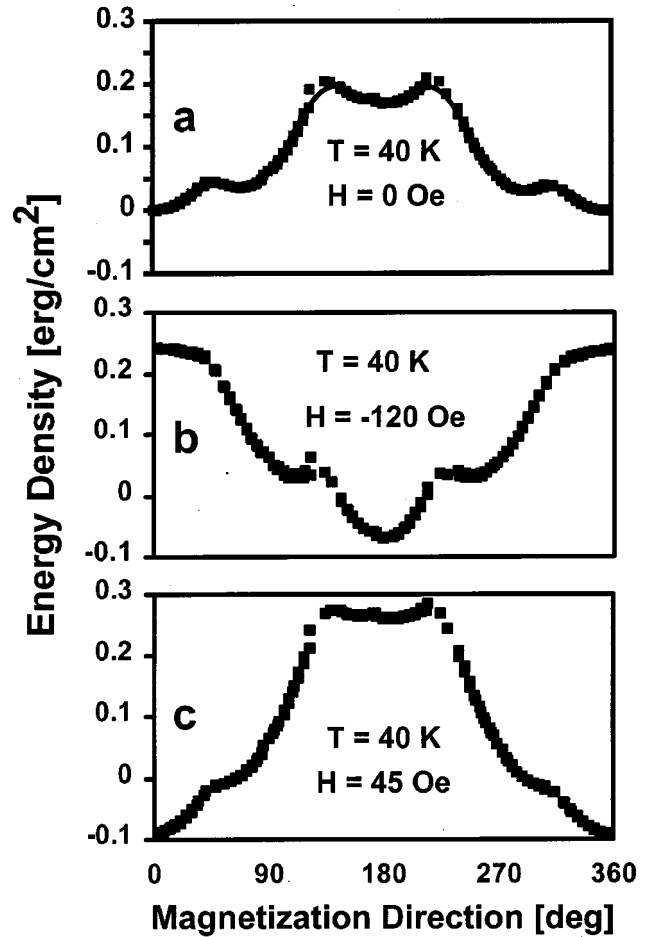


FIG. 4. Plots of the total energy of the Fe magnetization given by Eq. (3) for (a) no applied field and the two coercive fields: (b)  $-120$  Oe and (c)  $45$  Oe at  $T = 40$  K. The line in (a) is a fit of Eq. (4) to the experimental data. At the left coercive field (b), there are two local minima at nearly  $90^\circ$  to the applied field direction that promote magnetization reversal by two approximately  $90^\circ$  steps. The local minima are absent at the right coercive field (c), and therefore the reversal by a single  $180^\circ$  step is more favorable in this case.

note that the threefold anisotropy constant has the same order of magnitude as the uniaxial and the biaxial anisotropy constants and setting  $K_3$  equal to zero decreases the quality of the fit. On the contrary, the inclusion of higher order anisotropy terms [ $K_n \cos(n\alpha)$  with  $n > 4$ ] does not improve the fit and the corresponding anisotropy constants are more than a factor of ten smaller than  $K_3$ . Although our observation of the threefold symmetry may be somewhat surprising, it has been previously suggested in Ref. 17.

The presence of this threefold anisotropy term explains the asymmetry observed at the reversal field and shown in Fig. 4. Note that a combination of unidirectional, uniaxial and biaxial anisotropy components does not create magnetization reversal asymmetry. Indeed, a sample with only a uniaxial and a biaxial anisotropy components obviously has a symmetric hysteresis loop. If, in addition to the uniaxial and biaxial terms, there is a unidirectional anisotropy of the form  $K_{UD} \cos(\alpha)$ , then it can only result in a shift of the

hysteresis loop but cannot change its shape. This is because the functional form of the unidirectional anisotropy,  $K_{UD} \cos(\alpha)$ , is identical to that of the Zeeman energy,  $H_A \cdot M \cdot t_F \cos(\alpha)$ , in Eq. (3). Therefore, our hysteresis loop problem with the addition of the unidirectional anisotropy is algebraically equivalent to the problem of uniaxial and biaxial anisotropies only with the applied field replaced by an effective field  $H_{\text{eff}} = H_A + K_{UD}/M \cdot t_F$ . As a result of this algebraic equivalence, the shape of the hysteresis loop will not change, but the loop will be shifted by  $K_{UD}/M \cdot t_F$ . The magnetization reversal process will also remain symmetric. The broken symmetry at the coercive fields shown in Fig. 4 is due to the threefold anisotropy component, and this anisotropy is responsible for the asymmetric magnetization reversal. This is an important point as the previously suggested explanation<sup>5,18</sup> for the reversal asymmetry only considered uniaxial, fourfold and unidirectional anisotropies. These investigations were performed with techniques less sensitive to the threefold term, which becomes apparent in the measurements presented here. Our measurements provide a clear indication of this threefold anisotropy. This point is important as it has been demonstrated that the angular dependence of exchange bias and coercivity may have higher order terms ( $b_n \cos(n\alpha), n \geq 3$ ) in their Fourier expansion.<sup>19</sup> It was also shown that a Stoner-Wolfarth model that takes into account only simple uniaxial and unidirectional anisotropy components can produce an angular dependence of exchange bias and coercivity with such higher order terms.<sup>20</sup> Thus, the nontrivial angular dependence of exchange bias and coercivity does not necessarily imply a nontrivial angular dependence of the exchange anisotropy energy. Therefore, direct mea-

surements of the angular dependence of the exchange anisotropy energy, such as the measurements presented here, are necessary in order to establish the presence of the high order terms in its Fourier expansion. A possible origin of the threefold and uniaxial anisotropy terms is the nonrigid spin structure of the AF layer.<sup>21</sup> Rotation of the F layer magnetization may cause canting of the AF spins. It was theoretically shown<sup>21</sup> that these rotations of the AF spins away from an AF easy axis may lead to high order terms in the Fourier expansion of the exchange anisotropy.

In conclusion, we have measured the temperature dependence of the exchange anisotropy in Fe/MnF<sub>2</sub> bilayers. This anisotropy, induced by the F/AF exchange coupling, consists of a biaxial component, which gives rise to the enhanced coercivity,<sup>16</sup> a unidirectional component, which induces the hysteresis loop shift, a uniaxial component with its easy direction perpendicular to the easy direction of the unidirectional anisotropy, and a threefold symmetry component. We have found that the threefold component is responsible for the symmetry breaking in the magnetization reversal process. To our knowledge, this is the first direct experimental observation of a threefold exchange anisotropy term. Our results are consistent with and, more important, explain the origin of the magnetization reversal asymmetry recently observed by neutron reflectometry,<sup>5</sup> magnetometry,<sup>18</sup> and magneto-resistance<sup>8</sup> measurements in Fe/MnF<sub>2</sub> bilayers.

We would like to thank P. A. Crowell and R. Victora for helpful discussions. This work was supported by the University of Minnesota MRSEC, at UCSD by NSF and US DOE, and partial funding from the Catalan DGR (1999SGR00340) is also acknowledged.

- 
- <sup>1</sup>W. H. Meiklejohn and C. P. Bean, *Phys. Rev.* **102**, 1413 (1956).  
<sup>2</sup>J. Nogués and Ivan K. Schuller, *J. Magn. Magn. Mater.* **192**, 203 (1999).  
<sup>3</sup>B. Dieny, V. S. Speriosu, S. S. P. Parkin, B. A. Gurney, D. R. Wilhoit, and D. Mauri, *Phys. Rev. B* **43**, 1297 (1991).  
<sup>4</sup>V. I. Nikitenko, V. S. Gornakov, A. J. Shapiro, R. D. Shull, Kai Liu, S. M. Zhou, and C. L. Chien, *Phys. Rev. Lett.* **84**, 765 (2000).  
<sup>5</sup>M. R. Fitzsimmons, P. Yashar, C. Leighton, Ivan K. Schuller, J. Nogués, C. F. Majkrzak, and J. A. Dura, *Phys. Rev. Lett.* **84**, 3986 (2000).  
<sup>6</sup>Harsh Deep Chopra, David X. Yang, P. J. Chen, H. J. Brown, L. J. Swartzendruber, and W. F. Egelhoff, Jr., *Phys. Rev. B* **61**, 15 312 (2000).  
<sup>7</sup>X. Portier, A. K. Petford-Long, A. de Morais, N. W. Owen, H. Laidler, and K. O'Grady, *J. Appl. Phys.* **87**, 6412 (2000).  
<sup>8</sup>C. Leighton, M. Song, J. Nogués, M. C. Cyrille, and Ivan K. Schuller, *J. Appl. Phys.* **88**, 344 (2000).  
<sup>9</sup>E. D. Dahlberg, K. T. Riggs, and G. A. Prinz, *J. Appl. Phys.* **63**, 4270 (1988).  
<sup>10</sup>B. H. Miller and E. D. Dahlberg, *Appl. Phys. Lett.* **69**, 3932 (1996).  
<sup>11</sup>C. Leighton, J. Nogués, H. Suhl, and Ivan K. Schuller, *Phys. Rev. B* **60**, 12 837 (1999).  
<sup>12</sup>J. Nogués, D. Lederman, T. J. Moran, and Ivan K. Schuller, *Phys. Rev. Lett.* **76**, 4624 (1996).  
<sup>13</sup>P. Miltényi, M. Gruyters, G. Güntherodt, J. Nogués, and Ivan K. Schuller, *Phys. Rev. B* **59**, 3333 (1999).  
<sup>14</sup>C. Mathieu, M. Bauer, B. Hillebrands, J. Fassbender, G. Güntherodt, R. Jungblut, J. Kohlhepp, and A. Reinders, *J. Appl. Phys.* **83**, 2863 (1998).  
<sup>15</sup>N. C. Koon, *Phys. Rev. Lett.* **78**, 4865 (1997).  
<sup>16</sup>T. C. Schulthess and W. H. Butler, *Phys. Rev. Lett.* **81**, 4516 (1998).  
<sup>17</sup>Y. J. Tang, B. F. P. Roos, T. Mewes, A. R. Frank, M. Rickart, M. Bauer, S. O. Demokritov, B. Hillebrands, X. Zhou, B. Q. Liang, X. Chen, and W. S. Zhan, *Phys. Rev. B* **62**, 8654 (2000).  
<sup>18</sup>C. Leighton, M. R. Fitzsimmons, P. Yashar, A. Hoffmann, J. Nogués, J. Dura, C. F. Majkrzak, and Ivan K. Schuller, *Phys. Rev. Lett.* **86**, 4394 (2001).  
<sup>19</sup>T. Ambrose, R. L. Sommer, and C. L. Chien, *Phys. Rev. B* **56**, 83 (1997).  
<sup>20</sup>Haiwen Xi, Mark H. Kryder, and Robert M. White, *Appl. Phys. Lett.* **74**, 2687 (1999).  
<sup>21</sup>Joo-Von Kim, R. L. Stamps, B. V. McGrath, and R. E. Camley, *Phys. Rev. B* **61**, 8888 (2000).